ELSEVIER

1 November 1998

Optics Communications 156 (1998) 170–177

OPTICS COMMUNICATIONS

Full length article

A compact iodine-stabilized HeNe laser and crossover resonances at 543 nm

Wang-Yau Cheng [a,*], Jow-Tsong Shy [a], Tyson Lin [b]

[a] *Department of Physics, National Tsing Hua University, Hsinchu, Taiwan 300, ROC*
[b] *Physics Teaching and Research Center, Feng Chia University, Taichung, Taiwan 407, ROC*

Received 19 January 1998; revised 13 May 1998; accepted 22 July 1998

Abstract

We have constructed a compact iodine-stabilized 543 nm HeNe laser using the third-harmonic locking technique. From the signal-to-noise ratio, the noise-limited-stability would be better than 1×10^{-12} for integration time > 1 s. Moreover, several crossover resonances of R(12) 26–0 line are investigated and identified. Two crossover resonances are found adjacent to the hyperfine component a_9, the recommended wavelength standard. Instead, we suggest the hyperfine component b_{10} of R(106) 28–0 line as the wavelength standard for the absence of neighboring main lines or crossover resonances.

Keywords: Iodine-stabilization; 543 nm HeNe laser; Crossover resonance; Wavelength standard

1. Introduction

Since the redefinition of the basic unit of length in 1983 [1], the meter can be realized using the radiations of frequency-stabilized lasers locked to suitable atomic or molecular transitions [2]. At present, most national standard laboratories use the iodine-stabilized 633 nm HeNe laser to realize the meter. This laser is simple and compact, and many international comparisons have been performed [3,4]. Due to its weak absorption, the iodine cell is placed inside the laser cavity to increase the signal-to-noise ratio (S/N), and this introduces systematic errors to the accuracy of frequency, for instance, caused by nonlinearity of modulation, gas lensing, power broadening, etc. [5–7].

After the observation of saturation spectrum of iodine hyperfine transitions in an external absorption cell using an internal-mirror 543 nm HeNe laser in 1986 [8], there have been several iodine-stabilized 543 nm laser systems reported in the literature [9–14]. Both the third-harmonic locking technique and the frequency modulation spectroscopy method have been used to obtain the locking signal. The length of the extracavity iodine absorption cell varies from 30 to 120 cm. The best frequency stability achieved is 1×10^{-12} at 10 s integration time. Those systems are more complicated than the iodine-stabilized 633 nm laser systems and are not quite portable, therefore iodine-stabilized 543 nm laser systems are not commonly used and only one international comparison has been carried out up to now [14], although the iodine-stabilized 543 nm HeNe laser has been recommended as a wavelength standard since 1992 [15].

In this paper, we report a compact iodine-stabilized 543 nm HeNe laser system which is quite easy to maintain. In our setup, a short (6 cm long) iodine cell is used and the saturated absorption signals of the hyperfine structure are obtained using the standard third-harmonic demodulation technique. The saturation signal shows a $S/N \sim 8000$ at 1-Hz bandwidth for the a_9 component of the R(12) 26–0 line. Therefore the noise-limited-stability of the laser system locked to this resonance would be better than 1×10^{-12} after 1 s integration time. We have also measured the frequencies of several weak absorption lines and part of them are identified as the crossover resonances of the

* Corresponding author. E-mail: d827312@phys.nthu.edu.tw

0030-4018/98/$ - see front matter
PII: S0030-4018(98)00417-9

R(12) 26–0 line. Two crossover resonances are very close to the a_9 component and they can cause a shift of the locked laser frequency. The hyperfine component b_{10} of the R(106) 28–0 line would be a better reference line since there are no neighboring main lines or crossover resonances.

2. Experimental setup

The setup of our laser system is shown in Fig. 1. Three different 543 nm HeNe laser tubes are used in this experiment: Melles Griot 05LGR024, 05LGR024-S and 05LGR323, which have mode spacings of 750 MHz, 750 MHz and 556 MHz respectively. The 05LGR024 tube is filled with ^{20}Ne–^{22}Ne mixture with unknown ratio, 05LGR024-S is filled with ^{20}Ne, and 05LGR323 is filled with a 9:1 ^{20}Ne–^{22}Ne mixture. The differences between these three laser tubes are mode spacing, frequency tuning range and output power. The 05LGR323 laser has longer cavity length and hence higher output power. In addition, the 05LGR323 laser tube has three mode operation over a range of 200 MHz when one mode is near the center of the gain profile.

As shown in Fig. 1, the laser tube is mounted inside an aluminum tube for thermal shielding. Cavity misalignment caused by the thermal bending is serious for low gain laser tubes such as the 543 nm HeNe laser, therefore an alignment screw at the rear cavity mirror is used to optimize the output power. For modulating the laser frequency, a PZT tube is glued by epoxy onto the laser tube in between two aluminum rings. We achieve 35 MHz/V modulation width at the first mechanical resonance frequency of the laser tube (9.6 kHz) and 1 MHz/V frequency tuning at DC operation. We also wrap a thin heating film having 11 Ω resistance around the laser tube to control the laser cavity length. By applying a weak magnetic field over the laser tube at an angle of 45° to the natural axis of the laser tube, polarization flipping could be eliminated [16,17]. The laser output has a single mode tuning range of about 1 GHz and the maximum output power is 70 μW for 05LGR024 and 05LGR024-S laser tubes, and 120 μW output for 05LGR323 laser tube.

The overall length of our laser system is about 60 cm. The temperature of the cold finger of the 6 cm long iodine cell is kept at 0°C (corresponding iodine pressure is 4.12 Pa). The optical feedback is reduced by a Faraday isolator and a polarizing beam splitter (PBS) accompanied with a λ/4 waveplate. The optical isolation is better than 60 dB. The returned beam reflected by the PBS is detected by a photodiode and the saturation absorption spectrum is obtained by the third-harmonic demodulation technique. Unlike our previous work [13], the laser is modulated at a modulation frequency of 32 kHz which is not the mechanical resonance frequency of the laser tube. A PI (Proportional–Integral) feedback loop is used to control the laser frequency by adjusting the current of the heating film.

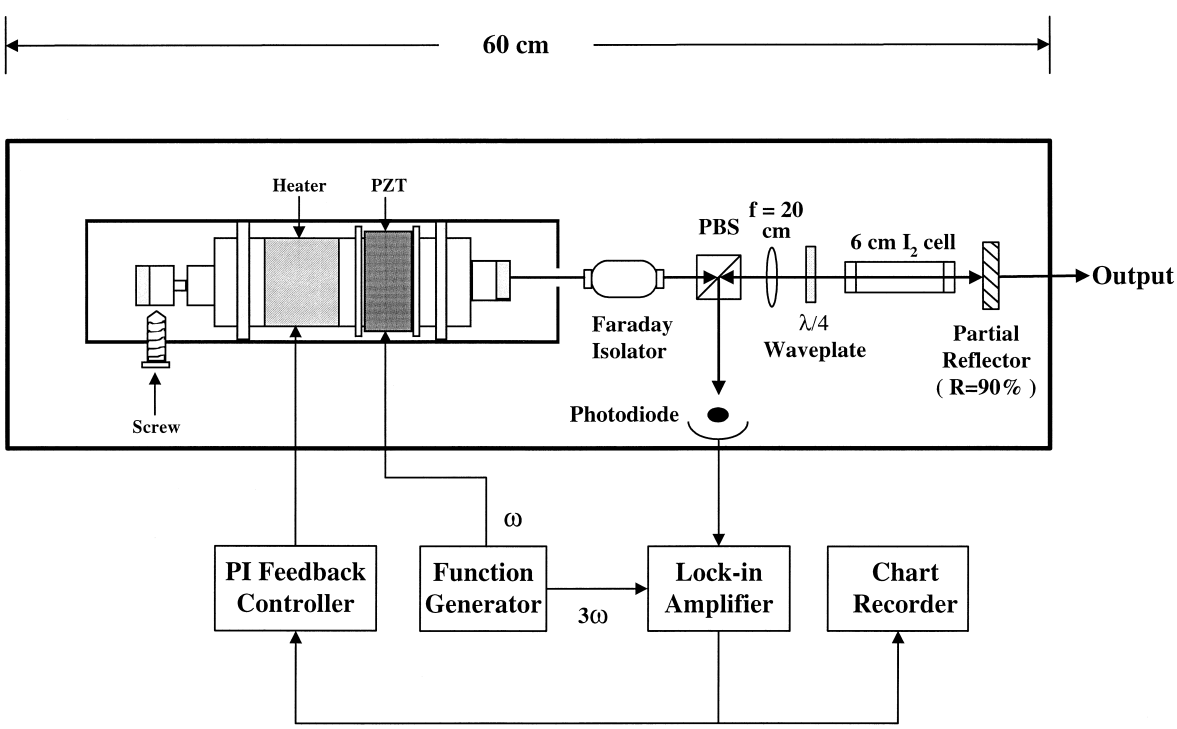

Fig. 1. Schematic diagram of the stabilized laser system. PBS: polarizing beam splitter.

Finally, for studying the effects of the modulation width on linewidth, S/N and sensitivity and for measuring the frequencies of weak absorption lines, beat-frequency measurements are carried out with a two-mode stabilized laser which has a stability of 1×10^{-11} at 1 s integration time and drift less than 1 MHz per day [18].

3. Results

The typical chart recorder traces of the saturated-absorption spectrum obtained with LGR-024 and LGR-323 laser tubes by thermal tuning are shown in Figs. 2 and 3 respectively. The spectrum obtained with LGR-024-S laser has the same feature except its tuning range covers from a_6 to b_9 components instead. The lock-in time constant is 3 ms. The modulation width is 3 MHz in Fig. 3 and the modulation width in Fig. 2 is 2 MHz to reduce the modulation broadening and increase the resolution. By this way we can easily resolve most weak transitions. The main lines with $\Delta F = \Delta J = +1$ are easily observed. Totally, we have observed 24 main lines, a_7 to a_{15} and b_1 to b_{15}. Here, a and b refer to R(12) 26–0 and R(106) 28–0 hyperfine lines, respectively. The main lines show excellent S/N due to high modulation frequency (32 kHz) in our experiment. The S/N of a_9 component is ~ 8000 normalized to 1 Hz bandwidth. Therefore, the noise-limited-stability of the laser locked to this line would theoretically be better than 1×10^{-12} for integration time > 1 s. This is better than our previous results [13] obtained

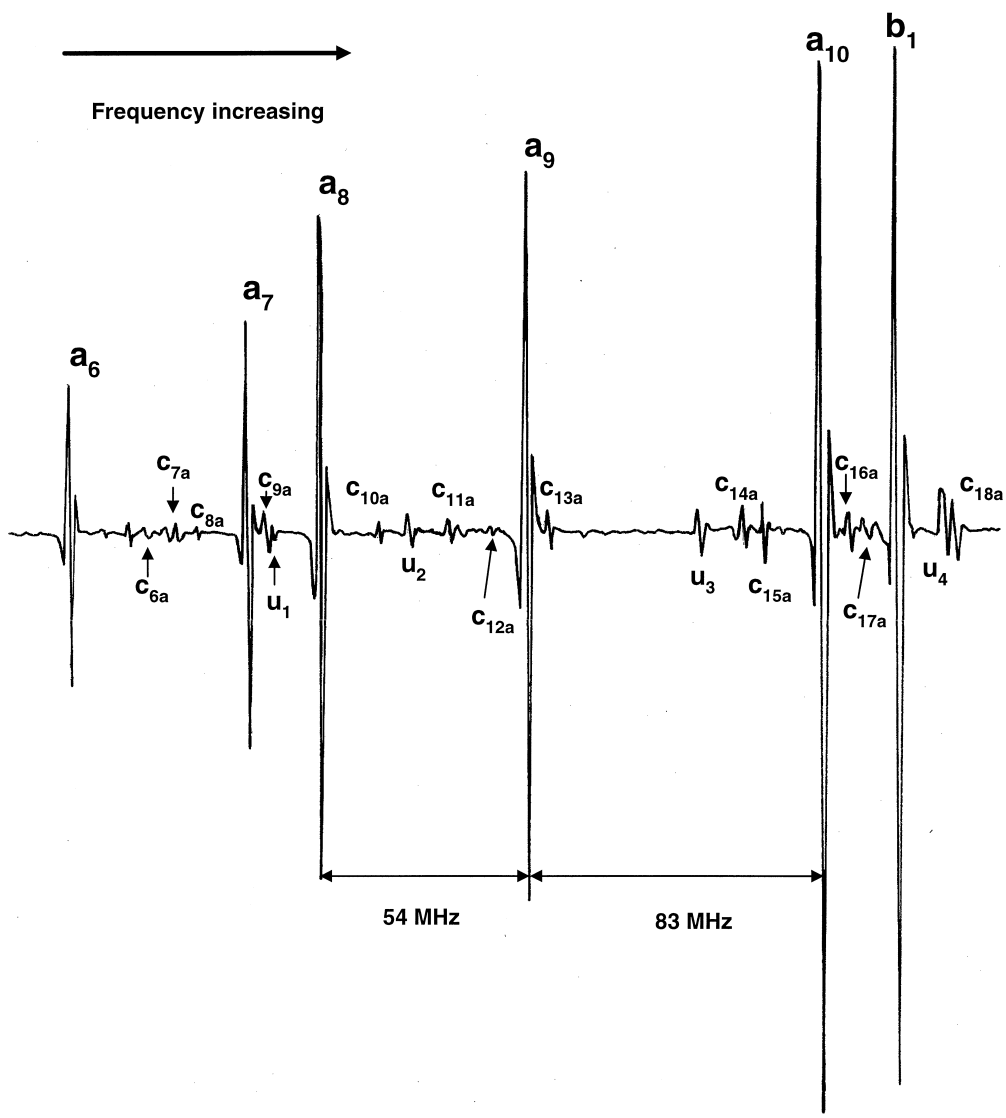

Fig. 2. Spectrum obtained with Melles Griot LGR323 laser. The time constant is 3 ms and modulation width is 2 MHz. The frequency scale is not linear.

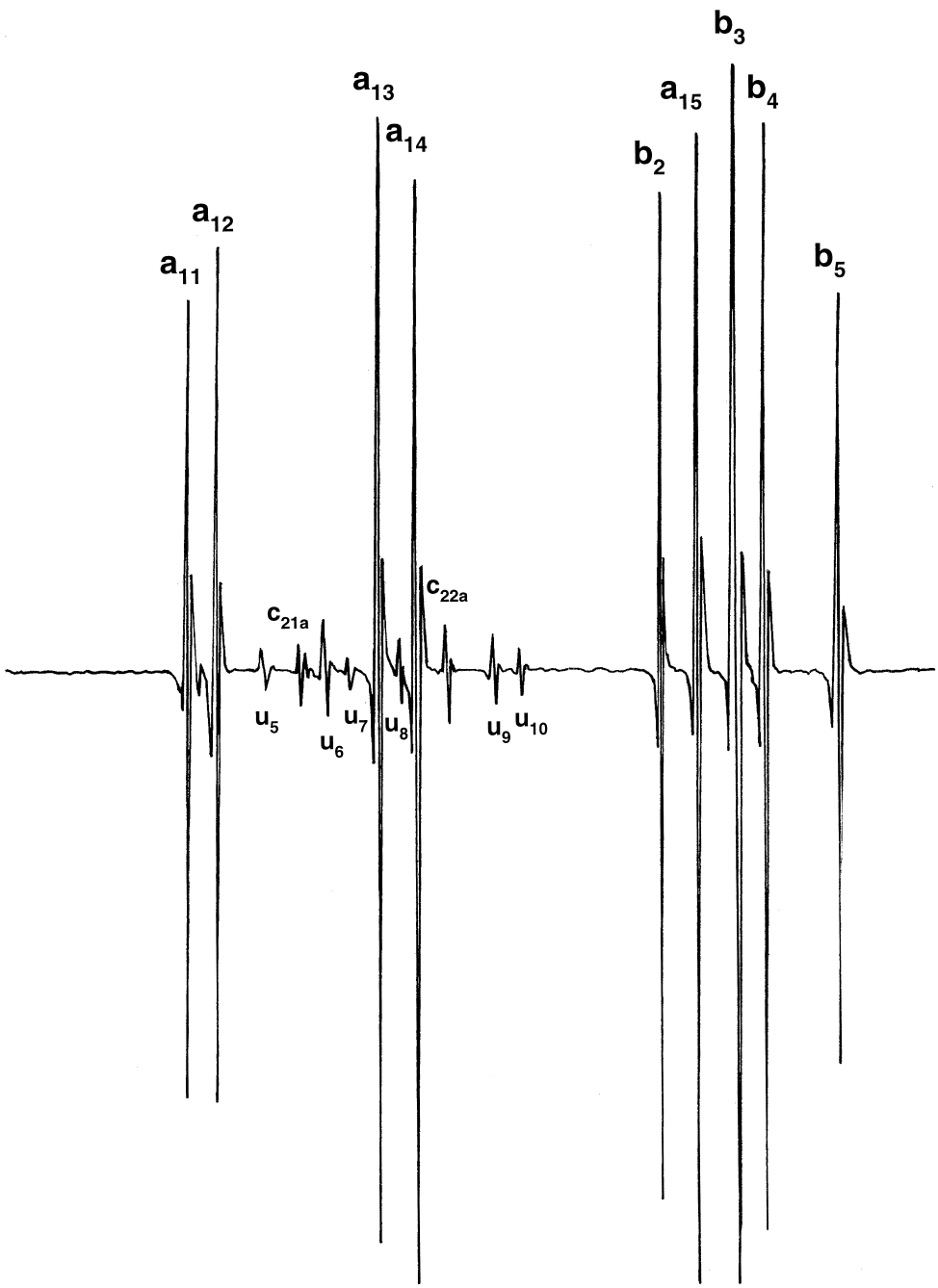

Fig. 2 (continued).

with a 120 cm long iodine cell. The laser can be locked to a_9 using only the thermal loop for more than five hours although it is in an ordinary laboratory with noisy background and without temperature regulation. The achieved frequency stability can be estimated from the fluctuations of the error signal to be 2×10^{-12} for averaging times > 1 s.

In addition to the main lines, there are many weak absorption lines. Most of the weak lines are located in the range of hyperfine structure of the R(12) 26–0. In order to identify those weak transitions, we lock alternately the laser to each weak line and measure its frequencies with respect to the above-mentioned two-mode stabilized laser. And the frequency of the two-mode stabilized laser is

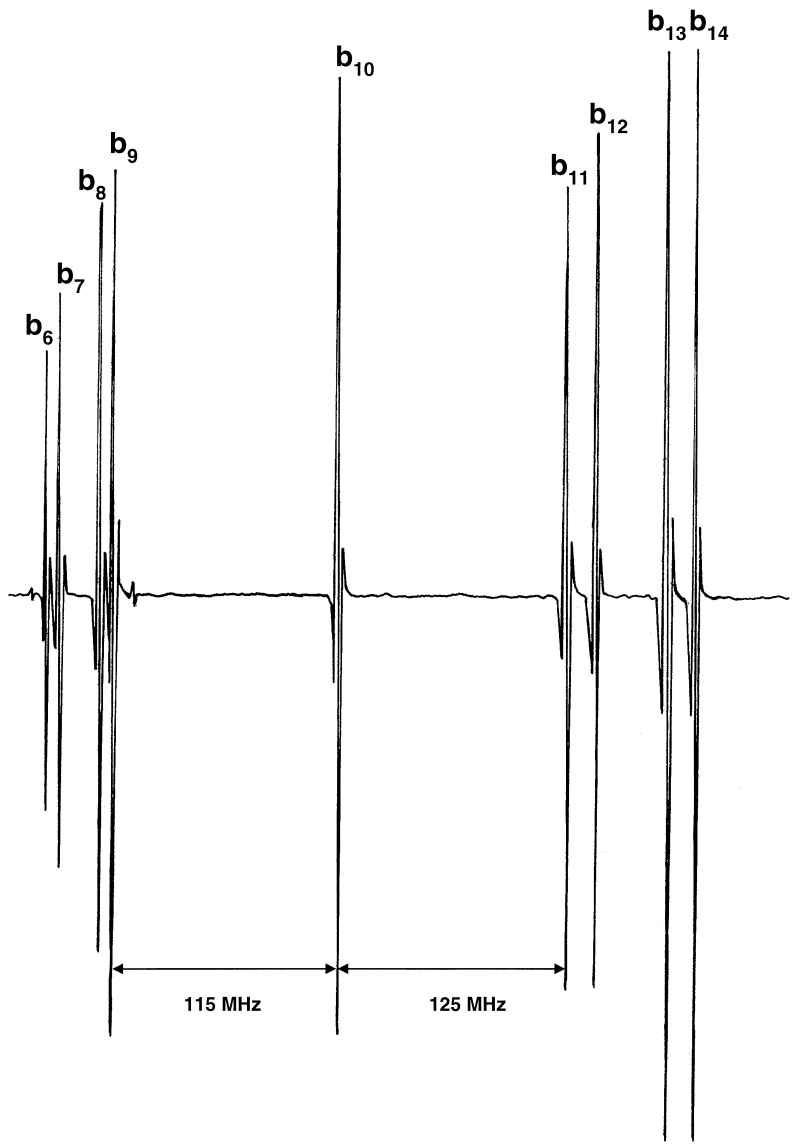

Fig. 2 (continued).

calibrated against an iodine-stabilized laser right after each measurement. Part of them can be identified as crossover resonances of the R(12) 26–0 line. The measured frequencies of the identified crossover resonances listed in Table 1 have good agreement with the theoretical calculation. The uncertainty of the measured frequencies (0.3 MHz) is mainly due to the drift of the reference laser, and the uncertainty of the theoretical frequencies is less than 0.1 MHz. The discrepancy between experimental data and theoretical frequencies is mainly due to the offset of the locking point by the nearby lines.

However, about half of the weak lines resolved are ambiguous in clarification. The possibility of impurities in the iodine cell is small because we find the same weak lines in different iodine cells from different sources. Therefore, we suspect that they belong to the hyperfine components of weak iodine transitions such as P(110) 35–2 and so on. The measured frequencies of the unidentified lines relative to a_9 are listed in Table 2. Please note there are two crossover resonances c_{12a} and c_{13a} close to the recommended wavelength standard transition a_9. On the contrary, the crossover resonances of R(106) 28–0 lines are unobservable. This is mainly due to its high rotational quantum number ($J = 106$) thus the transition cross-section of the dipole-forbidden line ($\Delta F = \Delta J = 0$) is diminished. In addition, the frequency intervals of b_{10} to its neighboring main lines (115 and 125 MHz) are larger than those of a_9 (54 and 83 MHz), thus the b_{10} component of

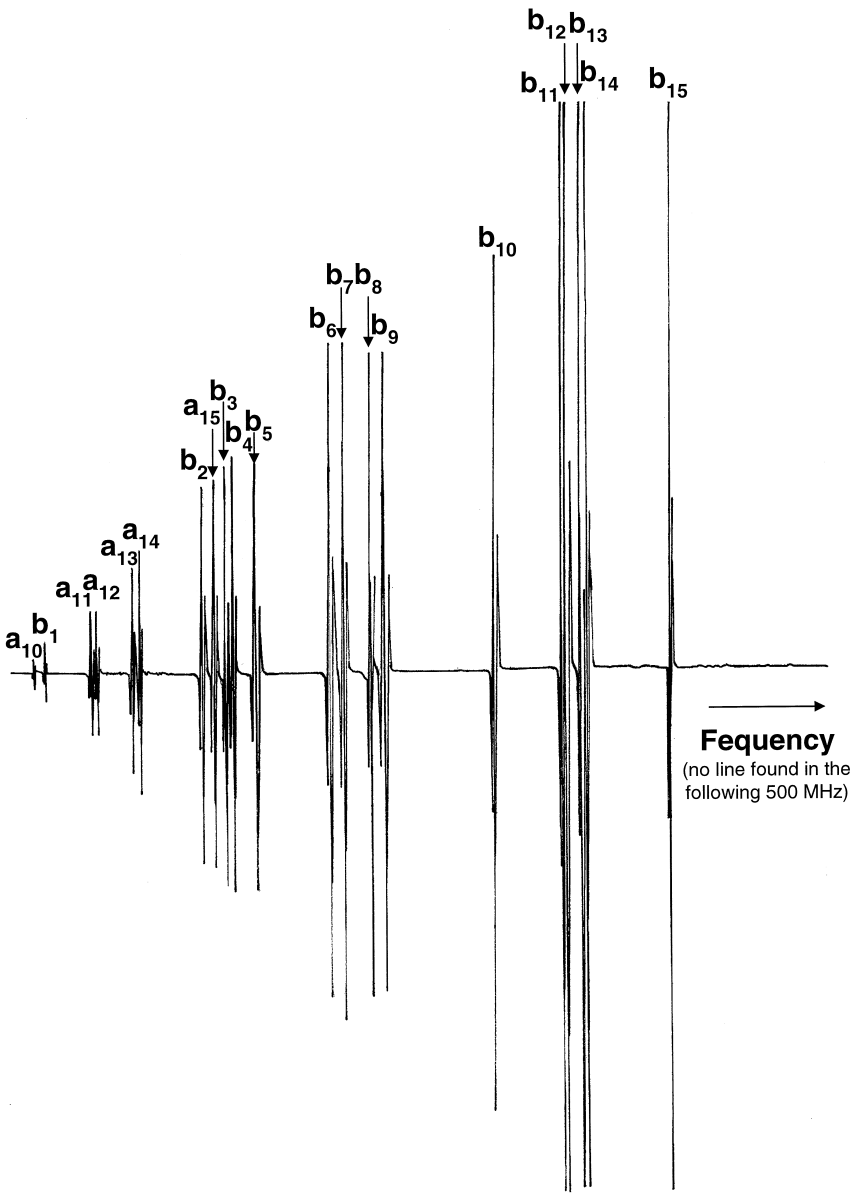

Fig. 3. Spectrum obtained with Melles Griot LGR024 laser. The time constant is 3 ms and modulation width is 3 MHz. The frequency scale is not linear.

the R(106) 28–0 line would be a better reference when setting up a wavelength standard. Therefore we suggest the b_{10} component as the wavelength standard in the future recommendation. Here we would like to remind the readers that the b_{10} line lies at the border of the emission range of 543 nm HeNe laser tubes filled with pure ^{20}Ne or ^{22}Ne isotope. However, one can easily find the b_{10} line using tubes filled with ^{20}Ne–^{22}Ne mixture as illustrated in Figs. 2 and 3.

We want to point out that most of the weak absorption lines observed in our previous work (see Fig. 2 of Ref. [13]) are probably due to unknown impurities in our 120 cm long iodine cell or due to another weak longitudinal mode. The laser used in our previous work had three-mode operation when one of the longitudinal modes was near the center of the gain profile. One of the two side modes had the same polarization as the central mode. Therefore, another weak longitudinal mode was presented in the laser beam after the PBS. (refer to Fig. 1 of Ref. [13]). To avoid the above mentioned problems, we compare the observed spectrum with the spectrum obtained using an iodine cell bought from Opthos Instrument Inc., U.S.A., and no differ-

Table 1
The identified crossover resonances of R(12) 26–0

Symbol	Identification	Frequency w.r.t. a_9 (MHz)	
		Measured	Theoretical
c_{6a}	$a_6 f_{5a}$ crossover	−100.7	−100.8
c_{7a}	$a_8 f_{4a}$ crossover	−97.2	−97.2
c_{8a}	$a_6 f_{6a}$ crossover	−89.8	−89.9
c_{9a}	$a_7 f_{6a}$ crossover	−67.9	−68.1
c_{10a}	$a_9 f_{5a}$ crossover	−38.1	−39.7
c_{11a}	$a_8 f_{7a}$ crossover	−20.4	−20.8
c_{12a}	$a_8 f_{8a}$ crossover	−6.5	−6.9
c_{13a}	$a_9 f_{7a}$ crossover	6.2	6.1
c_{14a}	$a_{12} f_{5a}$ crossover	60.4	57.7
c_{15a}	$a_{10} f_{8a}$ crossover	66.6	66.7
c_{16a}	$a_{14} f_{5a}$ crossover	91.9	91.2
c_{17a}	$a_{13} f_{6a}$ crossover	96.9	97.4
c_{18a}	$a_{11} f_{8a}$ crossover	122.2	121.9
c_{21a}	$a_{11} f_{9a}$ crossover	230.8	230.8
c_{22a}	$a_{13} f_{10a}$ crossover	279.5	279.4

Theoretical calculation is taken from Ref. [19]. Here, f stands for the dipole forbidden lines ($\Delta F = \Delta J = 0$). The differences between experimental data and theoretical frequencies are mainly due to the offset of the locking point by the nearby lines.

ences are found. We have also checked the frequency intervals between the weak lines and main lines and none of them equal to the laser mode spacing. Thus we believed that the weak lines are real iodine transitions.

As for studying the effects of the modulation width in our system, the MBW (modulation broadening width), S/N, and sensitivity versus the modulation width are studied and shown in Fig. 4. Here, the MBW is defined as the frequency difference between the two side zeros of the third derivative signal, S/N is the peak-to-peak signal divided by the noise, and sensitivity is the peak-to-peak signal divided by the MBW. The measured results compare very well with the analytical analysis by Nakazawa

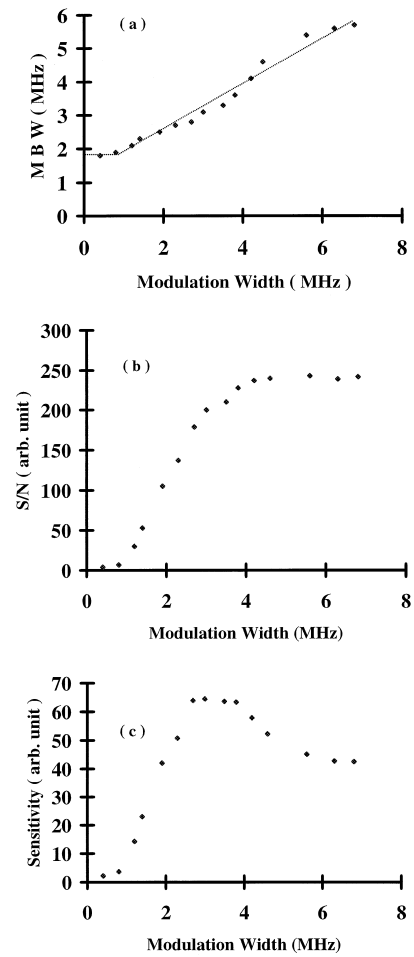

Fig. 4. The effects of modulation width in our system, all data are taken for a_9. MBW: modulation broadening width. (a) MBW versus modulation width. (b) S/N versus modulation width, and (c) sensitivity versus modulation width.

Table 2
The measured frequencies (w.r.t. a_9) of the unidentified weak lines

Symbol	Measured frequency w.r.t. a_9 (MHz)
u_1	−60.0
u_2	−31.1
u_3	−48.2
u_4	119.3
u_5	219.2
u_6	239.1
u_7	246.8
u_8	263.6
u_9	297.8
u_{10}	307.6

Their positions are illustrated in Fig. 2.

[20]. From Fig. 4(a) the modulation broadening is 0.76 ± 0.05 MHz/MHz (compare to 0.77 MHz/MHz from analytical analysis) and the FWHM of the iodine hyperfine peak a_9 (corresponding to the MBW at zero modulation width) is found to be 1.8 MHz in agreement with the result in Ref. [10] obtained at the iodine pressure of 2.2 Pa, and with the unpublished result by Rayman et al. [21] at an iodine pressure identical to ours. This indicates that the linewidth of the a_9 peak is not dominated by pressure broadening at our experimental conditions. It is worth noting that the FWHM obtained in Ref. [12] is about 0.9 MHz.

The S/N in our system increases with increasing modulation width as illustrated in Fig. 4(b). However, increasing modulation width also induces modulation broadening which will decrease the sensitivity in frequency stabilization. From Fig. 4(c) it is found that the maximum sensitiv-

ity occurs at modulation width of 3 MHz. The analytical analysis by Nakazawa [20] shows that the peak sensitivity occurs at modulation width equal to 1.64 times the FWHM of hyperfine peak; therefore the linewidth of the iodine hyperfine peaks is estimated to be 1.83 MHz which agrees with the FWHM obtained from Fig. 4(a).

4. Conclusions

We have constructed a compact iodine-stabilized 543 nm HeNe laser system which is simple to maintain and shows good S/N. The noise-limited-stability is estimated to be better than 1×10^{-12} for integration time > 1 s. At present only the slow thermal control loop is used to lock the laser. We believe that the noise-limited stability can be reached if a fast servo-loop using the PZT is also employed. The advantages of this system over the iodine-stabilized 633 nm laser system are better stability and less systematic shifts theoretically. Furthermore, several crossover resonances of R(12) 26–0 line are identified. Two crossover resonances are very close to the a_9 component and they can cause a shift of the laser frequency of these recommended wavelength standards. For this reason we propose to use the hyperfine component b_{10} instead of component a_9 as a reference component in setting up a wavelength standard at 543 nm wavelength. In the future, a systematic study on laser locked to b_{10} will be carried out and we also plan to perform inter comparison with other laboratories.

Acknowledgements

The authors wish to thank the support of the National Science Council of ROC under the contracts NSC84-2112-M-007-033 and NSC85-2112-M-007-037.

References

[1] Documents concerning the new definition of the meter, Metrologia 19 (1984) 163.
[2] BIPM Proc. Verb. Com. Int. Poids et Mesures 60, Recommendation 2 (CI-1992).
[3] M. Erin, B. Karaboce, I. Malinovsky, A. Titov, H. Ugur, H. Darnedde, F. Riehle, Metrologia 32 (1995) 301.
[4] J.-M. Chartier, A. Chartier, Metrologia 34 (1997) 297.
[5] G.R. Hanes, K.M. Baird, J. DeRemigis, J. Appl. Optics 12 (1973) 1600.
[6] P. Cerez, S.J. Bennett, Appl. Optics 18 (1979) 1079.
[7] J. Helmcke, F. Bayer-Helms, IEEE Trans. Instrum. Meas. IM–23 (1974) 529.
[8] J.-M. Chartier, J.L. Hall, M. Glaser, Proc. CPEM'86, 1986, p. 323.
[9] U. Brand, J. Helmcke, in: A. De Marchi (Ed.), Proc. Fourth Symposium on Frequency Standard and Metrology, Ancona, September 1988, Springer, Berlin, 1989, p. 467.
[10] J.-M. Chartier, S. Fredin-Picard, L. Robertsson, Optics Comm. 74 (1989) 87.
[11] H. Simonsen, O. Poulsen, Appl. Phys. B 50 (1990) 7.
[12] U. Brand, Optics Comm. 100 (1993) 361.
[13] T. Lin, Y.-W. Liu, W.-Y. Cheng, J.-T. Shy, B.-R. Jih, K.-L. Ko, Optics Comm. 107 (1994) 389.
[14] H.R. Simonsen, U. Brand, F. Riehle, Metrologia 31 (1995) 341.
[15] Mis en Pratique of the Definition of the Metre (1991), Metrologia 30 (1993/1994) 523.
[16] J.-T. Shy, C.-R. Yang, Appl. Optics 23 (1989) 4977.
[17] U. Brand, F. Mension, J. Helmeck, Appl. Phys. B 48 (1989) 343.
[18] W.-Y. Cheng, Y.-S. Chen, J.-T. Shy, T. Lin, Two-mode stabilized 543 nm HeNe laser using Bang–Bang control (unpublished).
[19] M. Glaser, Hyperfine components of iodine for optical frequency standards, PTB Bericht Opt-25.
[20] M. Nakazawa, J. Appl. Phys. 59 (1986) 2297.
[21] M.D. Rayman, M.P. Winters, J.L. Hall, private communication.